EFFECT OF PARTIAL SLIP FLOW AND HEAT TRANSFER OF NON - NEWTONIAN FLUID OVER A STRETCHABLE ROTATING POROUS DISK

Greeshma Joy

(Department of Mathematics, AJK College of Arts and Science, Tamilnadu, India)

ABSTRACT

In this article, the effect of partial slip flow and heat transfer of non - Newtonian fluid over a stretchable rotating porous disk is investigated. The solution of obtained equations is computed numerically using an Runge Kutta scheme. The numerical calculations for wall roughness parameter , Reiner - Rivlin fluid parameter are estimated. The effect of varied non - dimensional parameter wall roughness in Newtonian and non - Newtonian fluid, Reiner - Rivlin fluid, Prandtl number, thermal slip on velocity and temperature profile are analyzed through graphs.

Keywords : Von Karman flow, Heat Transfer, Non - Newtonian fluid, Partial Slip, Stretchable Rotating Disk

I INTRODUCTION

The steady incompressible flow induced by the rotation of an infinite plane with uniform angular rate is a certain resolution of the Navier – Stokes equations, as was initial described[1]. The flow is characterized by the dearth of a radial pressure gradient regarding the disk to balance the centrifugal forces therefore the fluid spirals outwards. The disk acts as a centrifugal fan, the fluid emanating from the disk being replaced by an axial flow directed back towards the surface of the disk. [2] explored stagnation-point flow because of stretchable rotating disk within the existence of thwart wise magnetic field. [3] extended from the quality Von Karman swirling flow problem wherever the rotating disk surface admits partial slip in the presence of a regular suction or injection.

The MHD steady flow of viscous Nano fluid because of a rotating disk has been investigated[4]. [5]enforced Keller - Box methodology for magneto Nano fluid flow and heat transfer close to a rotating disk to compute similarity solutions of the matter.[6] investigated numerical resolution of heat transfer analysis in three dimensional physical phenomenon stagnation point flow of incompressible ferro fluid over a stretchable rotating circular disk within the presence of uniform external field. Von Karman problem of infinite rotating disk was extended for the case wherever the area on top of the rough disk is provided by an electrically conducting nano fluid [7]. [8] explored the von - Karman problem for Bingham fluids. Their analysis unconcealed that yield stress in Bingham fluid contributes to a growth in minimum force required to keep up steady disk rotation. Non-Newtonian physical phenomenon flow and heat transfer over an exponentially stretching sheet with partial slip boundary condition has been studied [9].

The work [10], the Coupled flow and heat transfer in elastic fluid with Cattaneo - Christov heat flux model with the help of homotopy analysis methodology (HAM). In porous medium, the flow and radiation heat transfer of a nanofluid over a stretching sheet with velocity slip and temperature jump was mentioned[11]. [12] investigated a mixed convection flow of a third - grade fluid close to the orthogonal stagnation point on a vertical surface with slip and viscous dissipation effects. The boundary layer flow of a second-grade fluid during a porous medium past a stretching sheet and heat transfer characteristics with power-law surface temperature or heat flux was studied by [13].

[14] explored the heat transfer characteristics within the peristaltic transport of Powell-Eyring fluid within a semicircular channel with complaint walls. The streamline flow of Oldroyd-B fluid evoked by a deforming sheet within the existence of transversal magnetic flux was mentioned by [15]. Therefore the target of this present work is to the effect of partial slip flow and heat transfer of non - Newtonian Reiner - Rivlin fluid over a stretchable rotating disk. This present work is likely to possess concerning to the problem of heat transfer which may be helpful in industries for electrochemical systems, deposition of coatings on surfaces, rotor-stator system etc.

II MATHEMATICAL FORMULATION

Let the steady flow of an incompressible Reiner-Rivlin fluid occupying semi-infinite region on top of an infinite disk coinciding with the plane z = 0. The disk is during a state of rigid body rotation regarding the vertical axis with constant angular velocity ω through a porous medium that sets up a swirling flow within the neighboring fluid layers.

Let u, v and w be the elements of velocity on the directions of accelerating r, ϕ and z severally. Due to the axial symmetry, the velocity elements are assumed to be independent of the angle coordinate u. Partial slip conditions are enforced considering that characteristic scale of protuberance is tiny compared to the boundary layer thickness. Let T_W be the constant temperature at the disk and T_∞ is that the fluid temperature high above the surface. We tend to make use of the temperature jump condition is that the current analysis. Reiner and Rivlin have developed the subsequent represent relation:

$$\tau_{ij} = -p\delta_{ij} + \mu e_{ij} + \mu_c e_{ik} e_{kj} \; ; \qquad e_{jj} = 0, \tag{1}$$

in which τ_{ij} denotes the strain tensor, p represents pressure, μ is that the co-efficient of viscosity, μ_c represents the cross-viscosity constant, δ_{ij} is that the Kronecker symbol and $e_{ij} = \left(\frac{\partial u_i}{\partial x_j}\right) + \left(\frac{\partial u_j}{\partial x_i}\right)$ is that the deformation rate tensor. Relevant equations describing fluid motion and heat transfer over a rotating disk are given below:

Continuity Equation

$$\frac{\partial u}{\partial r} + \frac{u}{r} + \frac{\partial w}{\partial z} = 0 \tag{2}$$

Motion Equation

$$\rho\left(u\frac{\partial u}{\partial r}+w\frac{\partial u}{\partial z}-\frac{v^2}{r}\right)=\frac{\partial \tau_{rr}}{\partial r}+\frac{\partial \tau_{rz}}{\partial z}+\frac{\tau_{rr}-\tau_{\phi\phi}}{r} \tag{3}$$

$$\rho\left(u\frac{\partial v}{\partial r}+w\frac{\partial v}{\partial z}+\frac{uv}{r}\right)=\frac{1}{r^2}\frac{\partial}{\partial r}\left(r^2\tau_{r\phi}\right)+\frac{\partial \tau_{z\phi}}{\partial z}+\frac{\tau_{r\phi}-\tau_{\phi r}}{r} \tag{4}$$

$$\rho\left(u\frac{\partial w}{\partial r}+w\frac{\partial w}{\partial z}\right)=\frac{1}{r}\frac{\partial(r\tau_{rz})}{\partial r}+\frac{\partial \tau_{zz}}{\partial z} \tag{5}$$

Energy Equation

$$\rho c_p\left(u\frac{\partial T}{\partial r}+w\frac{\partial T}{\partial z}\right)=k\frac{\partial^2 T}{\partial z^2}, \tag{6}$$

where ρ stands for fluid density, k for thermal conduction and c_p for the specific heat capacity. The last term in Eq. (4) are often omitted by using symmetry assumption for the elements of stress tensor. For the current (axisymmetric) flow, the elements of deformation rate tensor are given below [8]:

$$\left.\begin{aligned} &e_{rr}=2\frac{\partial u}{\partial r}, \qquad e_{\phi\phi}=2\frac{u}{r}, \qquad e_{zz}=2\frac{\partial w}{\partial z}, \\ &e_{r\phi}=e_{\phi r}=r\frac{\partial}{\partial r}\left(\frac{v}{r}\right), \qquad e_{z\phi}=e_{\phi z}=\frac{\partial v}{\partial z}, \\ &e_{rz}=e_{zr}=\frac{\partial u}{\partial z}+\frac{\partial w}{\partial r} \end{aligned}\right\} \tag{7}$$

Through definition (1), the elements of stress tensor are obtained as follows:

$$\tau_{rr}=-p+\mu\left(2\frac{\partial u}{\partial r}\right)+\mu_c\left\{4\left(\frac{\partial u}{\partial r}\right)^2+\left(\frac{\partial v}{\partial r}-\frac{v}{r}\right)^2+\left(\frac{\partial u}{\partial z}+\frac{\partial w}{\partial r}\right)^2\right\} \tag{8}$$

$$\tau_{zr}=\mu\left(\frac{\partial u}{\partial z}+\frac{\partial w}{\partial r}\right)+\mu_c\left\{\left(2\frac{\partial u}{\partial r}\right)\left(\frac{\partial u}{\partial z}+\frac{\partial w}{\partial r}\right)+\left(\frac{\partial v}{\partial r}-\frac{v}{r}\right)\left(\frac{\partial v}{\partial z}\right)+\left(\frac{\partial u}{\partial z}+\frac{\partial w}{\partial r}\right)\left(2\frac{\partial w}{\partial z}\right)\right\} \tag{9}$$

$$\tau_{\phi\phi}=-p+\mu\left(2\frac{u}{r}\right)+\mu_c\left\{4\left(\frac{u}{r}\right)^2+\left(\frac{\partial v}{\partial r}-\frac{v}{r}\right)^2+\left(\frac{\partial v}{\partial z}\right)^2\right\} \tag{10}$$

$$\tau_{r\phi}=\mu\left(\frac{\partial v}{\partial r}-\frac{v}{r}\right)+\mu_c\left\{\left(2\frac{\partial u}{\partial r}\right)\left(\frac{\partial v}{\partial r}-\frac{v}{r}\right)+\left(\frac{\partial v}{\partial r}-\frac{v}{r}\right)\left(\frac{2u}{r}\right)+\left(\frac{\partial u}{\partial z}+\frac{\partial w}{\partial r}\right)\left(\frac{\partial v}{\partial z}\right)\right\} \tag{11}$$

$$\tau_{z\phi}=\mu\left(\frac{\partial v}{\partial z}\right)+\mu_c\left\{\left(\frac{\partial v}{\partial r}-\frac{v}{r}\right)\left(\frac{\partial u}{\partial z}+\frac{\partial w}{\partial r}\right)+2\left(\frac{u}{r}\right)\left(\frac{\partial v}{\partial z}\right)+2\left(\frac{\partial v}{\partial z}\right)\left(\frac{\partial w}{\partial z}\right)\right\} \tag{12}$$

$$\tau_{zz}=-p+\mu\left(2\frac{\partial w}{\partial z}\right)+\mu_c\left\{\left(\frac{\partial u}{\partial z}+\frac{\partial w}{\partial r}\right)^2+\left(\frac{\partial v}{\partial z}\right)^2+4\left(\frac{\partial w}{\partial z}\right)^2\right\} \tag{13}$$

The partial slip condition for present flow is expressed as follows by assumptive no penetration at the disk.

$$u(r,0)=\beta_1\tau_{rz}(r,0), \qquad v(r,0)=\beta_2\tau_{z\phi}(r,0)+r\omega, \qquad w=w_0$$

$$T(r,0)=T_w+\beta_3 T_z(r,0). \tag{14a}$$

in which β_1 denotes the radial slip coefficient, β_2 is the azimuthal slip coefficient and γ represents the thermal slip coefficient. Since lateral velocities and temperature distinction are zero removed from the disk thus we have

$$u(r,z)\to 0, \qquad v(r,z)\to 0. \qquad T(r,z)\to T_\infty \ \ as\ z\to\infty \tag{14b}$$

Let us outline the subsequent self-similar transformations in terms of dimensionless distance $\varsigma = (\omega/v)^{1/2}$

$$(u, v, w) = \left(r\omega F'(\varsigma), r\omega G(\varsigma), -2\sqrt{v\omega}F(\varsigma)\right)$$

$$(p, T) = \left(p_\infty - \omega\mu P(\varsigma), T_\infty + (T_W - T_\infty)\theta(\varsigma)\right), \quad (15)$$

where prime indicates differentiation with respect to ς. Note that Eq. (2) is identically satisfied by transformations (15) and (3) convert into the subsequent ordinary differential equations

$$F''' - F'^2 + 2FF'' + G^2 + K\left(F''^2 - 2F'F''' - G'^2\right) = 0 \quad (16)$$

$$G'' - 2F'G + 2FG' + 2K(F''G' - F'G'') = 0 \quad (17)$$

$$\theta'' + 2PrF\theta' = 0 \quad (18)$$

In the above equations, $pr = \frac{\mu C_p}{k}$ denotes the Prandtl number and $K = \frac{\mu_c \omega}{\mu}$ is material parameter of Reiner-Rivlin fluid. Let us define:

$$\lambda_1 = \rho(\omega v)^{1/2}\beta_1, \quad \lambda_2 = \rho(\omega v)^{1/2}\beta_2, \quad \gamma = \rho(\omega v)^{1/2}\beta_3 \quad (19)$$

Using (15), the boundary conditions (14a) and (14b) transform into the subsequent forms:

$$\left.\begin{aligned} F'(0) &= \lambda_1[F''(0) - 2KF'(0)F''(0)] \\ G(0) &= \lambda_2[G'(0) - 2KG'(0)F'(0)] + 1 \\ \theta(0) &= 1 + \gamma\theta'(0) \end{aligned}\right\} \quad (20a)$$

$$F' \to 0, G \to 0, \theta \to 0 \; as \; \varsigma \to \infty \quad (20b)$$

The presence of viscosity close to the disk produces tangential stress at the disk that resists its rotation. Torque T_0 required to keep up steady rotation of disk with radius R is measured through the definite integral.

$$T_0 = -\int_0^R \tau_{z\phi}|_{z=0}\,(2\pi r^2)dr = -\frac{\pi\rho\omega}{2}\sqrt{v\omega}R^4G'(0) \quad (21)$$

Quantity of prime interest during this work is that the skin friction coefficient C_f outlined as

$$C_f = \frac{\sqrt{\tau_r^2 + \tau_\phi^2}}{\rho(r\omega)^2} \quad (22)$$

where τ_r and τ_ϕ denote the radial and azimuthal wall stresses. Through variables (15), Eq. (22) assumes the subsequent form:

$$C_f = \left(\frac{\omega r^2}{v}\right)^{-1/2}\sqrt{\left(F''(0)\right)^2 + \left(G'(0)\right)^2} \quad (23)$$

Another necessary quantity is the local Nusselt number Nu which may be obtained from the Fourier law as follows:

$$Nu = \frac{rq_w}{k(T_W - T_\infty)} = \left(\frac{\omega r^2}{v}\right)^{1/2}\theta'(0) \quad (24)$$

Additionally, the overall quantity of fluid drawn within the axial direction is measured through $F(\infty)$. Therefore numerical computations for $F''(0), G'(0), \theta'(0)$ and $F(\infty)$ will be made to grasp physical aspects of the problem.

III NUMERICAL APPROACH

Mathematical equations are obtained in terms of higher order equation. Reduction of partial differential equation to nonlinear ordinary differential equation by exploitation some appropriate transformation.

The governing equations exhibit by (16) - (18) along with the conditions (20a) and (20b) could be a two-point boundary value problem that seems difficult to evaluate analytically. Therefore we tend to take Runge - Kutta methodology to seek a numerical resolution of the problem. Let us convert Eqs (16) - (18) into a system of first-order equations by substituting

$x_1 = F\ , x_2 = F'\ , x_3 = F''\ , x_4 = G\ \ , x_5 = G'\ , x_6 = \theta\ , x_7 = \theta'$

We acquire the subsequent

$$x_1' = x_2\ , \qquad x_2' = x_3\ , \qquad x_3' = \frac{x_2^2 - 2x_1x_3 - x_4^2 - Kx_3^2 + Kx_5^2}{1 - 2Kx_2}$$

$$x_4' = x_5, \qquad x_5' = \frac{2x_2x_4 - 2x_1x_5 - 2Kx_3x_5}{1 - 2Kx_2}$$

$$x_6' = x_7\ , \qquad x_7' = -2Prx_1x_7 \qquad (25)$$

With the initial conditions

$x_1(0) = 0\ ,$

$x_2(0) = \lambda_1[x_3(0) - 2Kx_2(0)x_3(0)]\ ,$

$x_3(0) = u(1)\ ,$

$x_4(0) = \lambda_2[x_5(0) - 2Kx_5(0)x_2(0)] + 1\ ,$

$x_5(0) = u(2),$

$x_6(0) = 1 + \gamma x_7(0),$

$x_7(0) = u(3) \qquad (4.26)$

To solve the above system numerically, we tend to implement Runge - Kutta methodology of fifth order considering appropriate guesses for the unknown slopes u(1), u(2) and u(3). Within the course of computations, the step size h = 0.01 is chosen whereas residual of boundary conditions at infinity is assumed to be 10^{-5}.

IV FIGURES AND TABLES

Table 1: Comparison of present findings with those of Turkyilmazoglu [2] in uniform roughness case $(\lambda_1 = \lambda_2)$ with K=0

λ_1	λ_2	Existing $F''(0)$	Existing $G'(0)$	Existing $F(\infty)$	Present $F''(0)$	Present $G'(0)$	Present $F(\infty)$
0	0	0.5102330	-0.6159218	0.442226	0.5102335	-0.6159214	0.442224
1	1	0.1279239	-0.3949279	0.394711	0.1279244	-0.3949274	0.394708
5	5	0.0185881	-0.1433878	0.291840	0.0185886	-0.1433873	0.291837
10	10	0.0068123	-0.0810300	0.243795	0.0068128	-0.0810297	0.243793
20	20	0.0023613	-0.0437882	0.199903	0.0023618	-0.0437878	0.199901
40	40	0.0007897	-0.0229950	0.160962	0.0007903	-0.0229946	0.160957

Table 2: Computational results of $F''(0), G'(O), F(\infty)$ and $\sqrt{(F''(0))^2 + (G'(0))^2}$ for different values of λ_1, λ_2 and K

λ_1	λ_2	K	$F(\infty)$	$F''(0)$	$G'(O)$	$\sqrt{(F''(0))^2 + (G'(0))}$
0	1	1	0.311703	0.207328	-0.358182	0.413859
1	1	1	0.344450	0.115542	-0.434950	0.450035
5	1	1	0.370577	0.046256	-0.495400	0.497559
10	1	1	0.377728	0.0269280	-0.512592	0.513298
20	1	1	0.382160	0.014732	-0.523513	0.523720
40	1	1	0.384367	0.007742	-0.529792	0.529848
1	0	1	0.391593	0.164950	-0.815801	0.832310
1	1	1	0.344450	0.115542	-0.434948	0.450033
1	5	1	0.259794	0.053218	-0.149822	0.158993
1	10	1	0.217802	0.033267	-0.083026	0.089443
1	20	1	0.164478	0.019743	-0.044249	0.048454
1	40	1	0.130637	0.011338	-0.023053	0.025688
1	1	0	0.394628	0.127917	-0.394920	0.415120
1	1	2	0.292082	0.077913	-0.424418	0.431510
1	1	4	0.224868	0.033992	-0.351566	0.353209
1	1	6	0.187209	0.020208	-0.304637	0.305308
1	1	8	0.166736	0.014228	-0.272426	0.272797

Table 3:Values of $\theta'(0)$ for different values of K, γ and Pr when $\lambda_1 = \lambda_2 = 1$

K	γ	Pr	$\theta'(0)$
0	1	8	0.533148
2	1	8	-0.453107
4	1	8	-0.370246
6	1	8	-0.322058
8	1	8	-0.289546
1	0	8	-1.003957
1	1	8	-0.500983
1	5	8	-0.166771
1	10	8	-0.090934
1	20	8	-0.047624
1	40	8	-0.024387
1	1	3	-0.343426

1	1	4	-0.394305
1	1	8	-0.500984
1	1	11	-0.544935

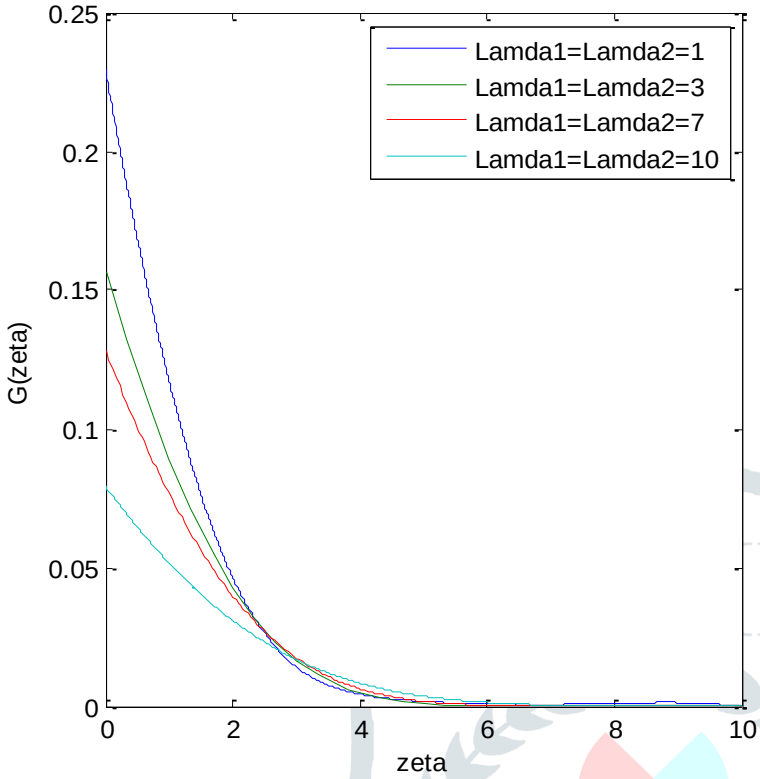

Figure 4.1 Velocity profile for different values of wall roughness parameters λ_1 and λ_2 in Newtonian fluid case

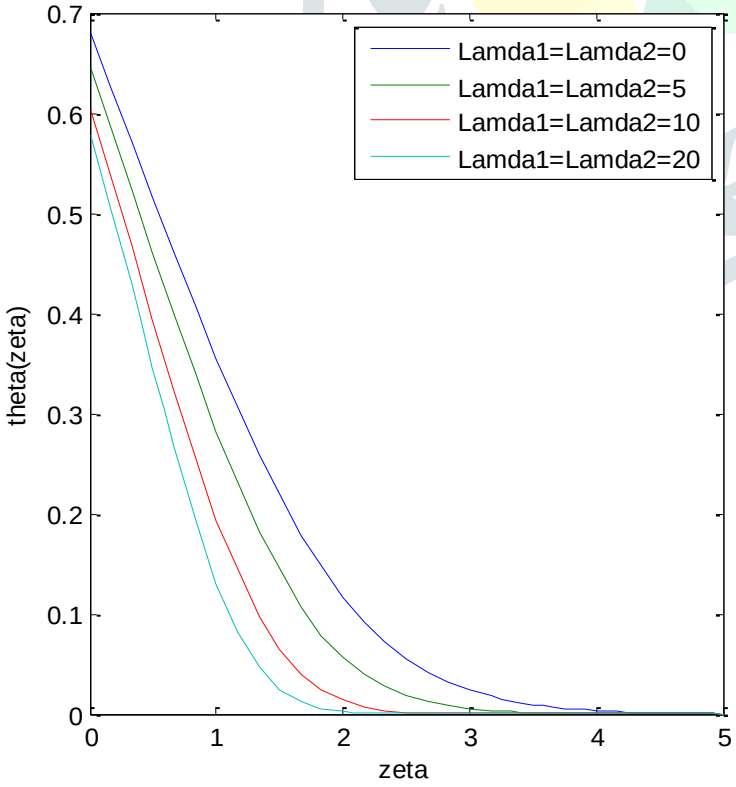

Figure 4.2 Temperature profile for different values of wall roughness parameters λ_1 and λ_2 in Newtonian fluid case

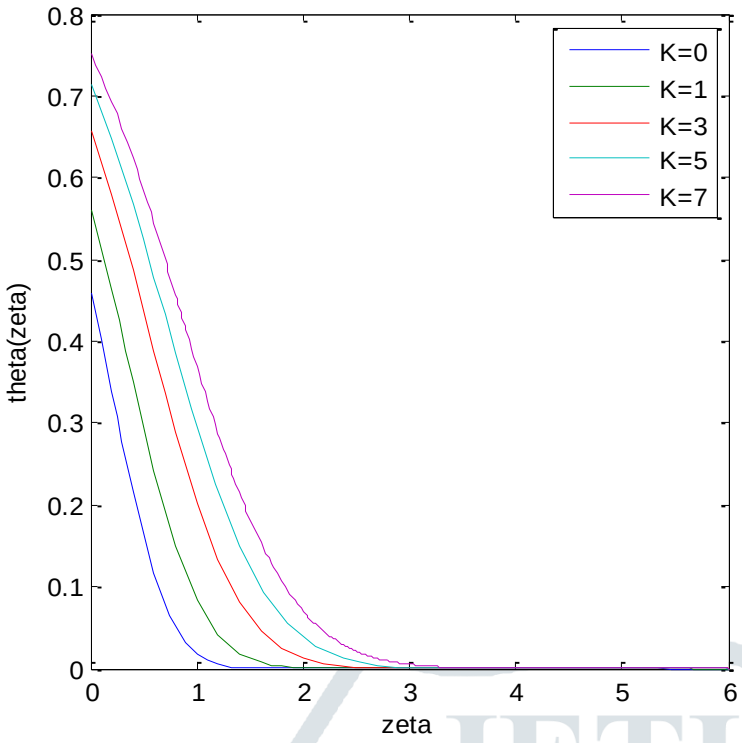

Figure 4.3 Temperature profile for different values of Reiner - Rivlin fluid parameter K

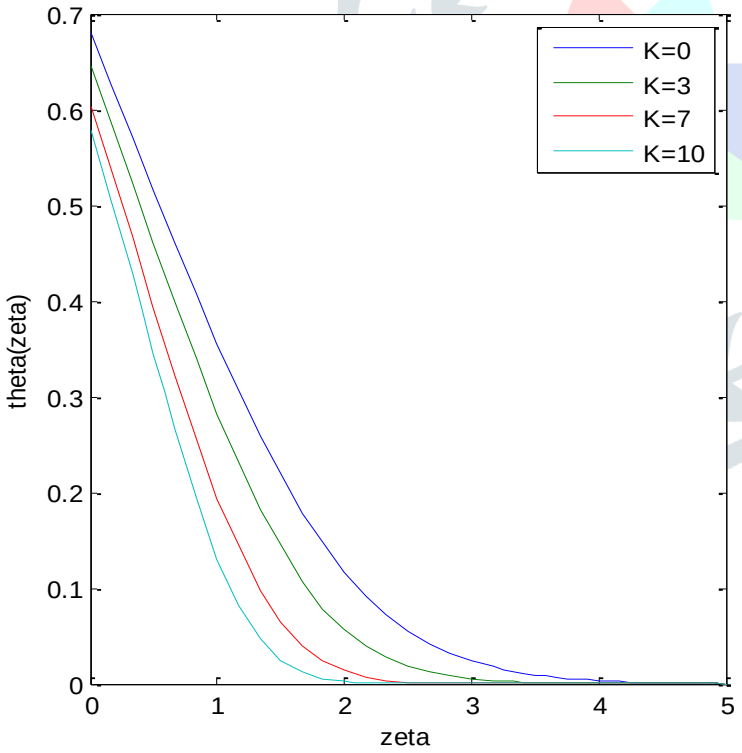

Figure 4.4 Temperature profile for different values of Reiner - Rivlin fluid parameter K in no - slip case

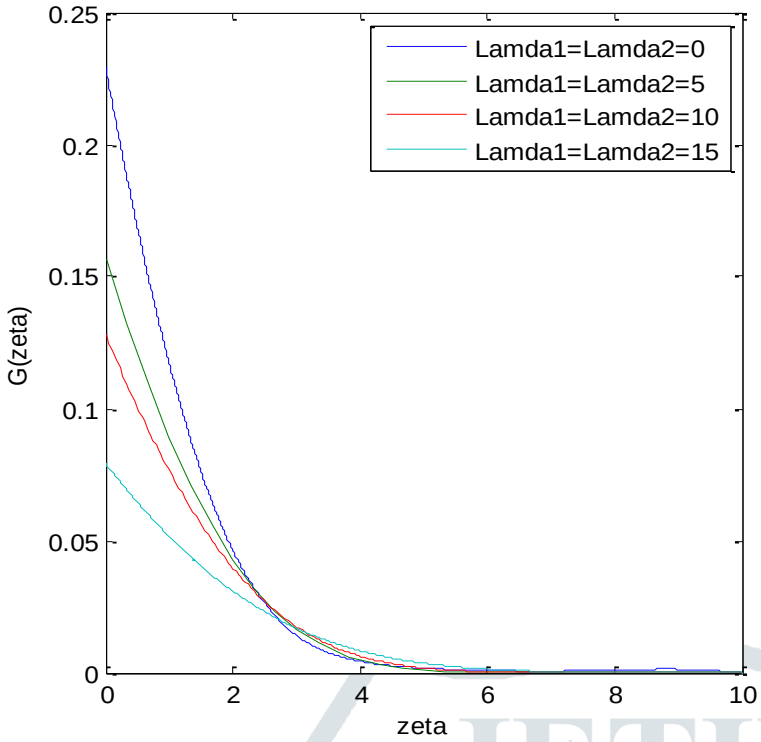

Figure 4.5 Velocity profile for different values of wall roughness parameters λ_1 and λ_2 in non - Newtonian fluid case

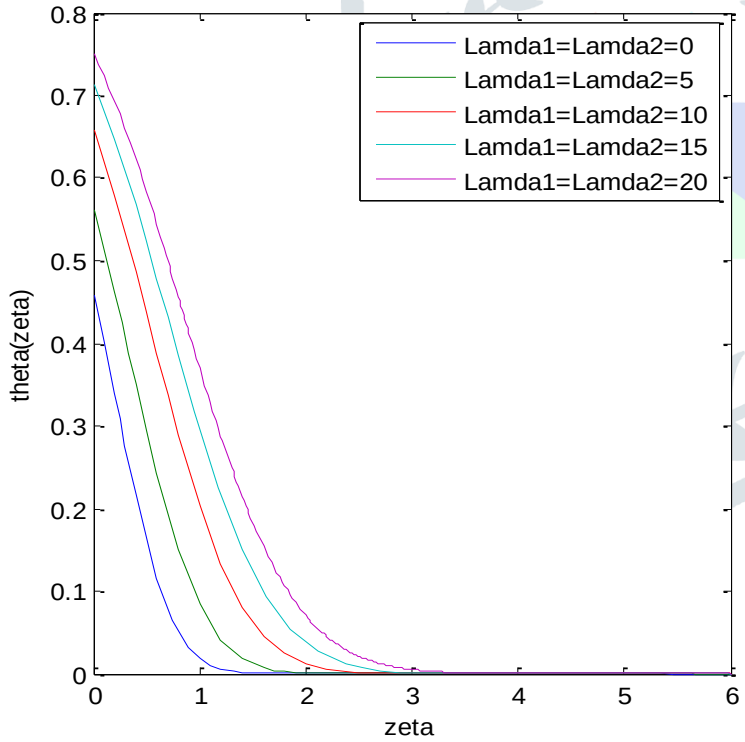

Figure 4.6 Temperature profile for different values of wall roughness parameters λ_1 and λ_2 in non - Newtonian fluid case

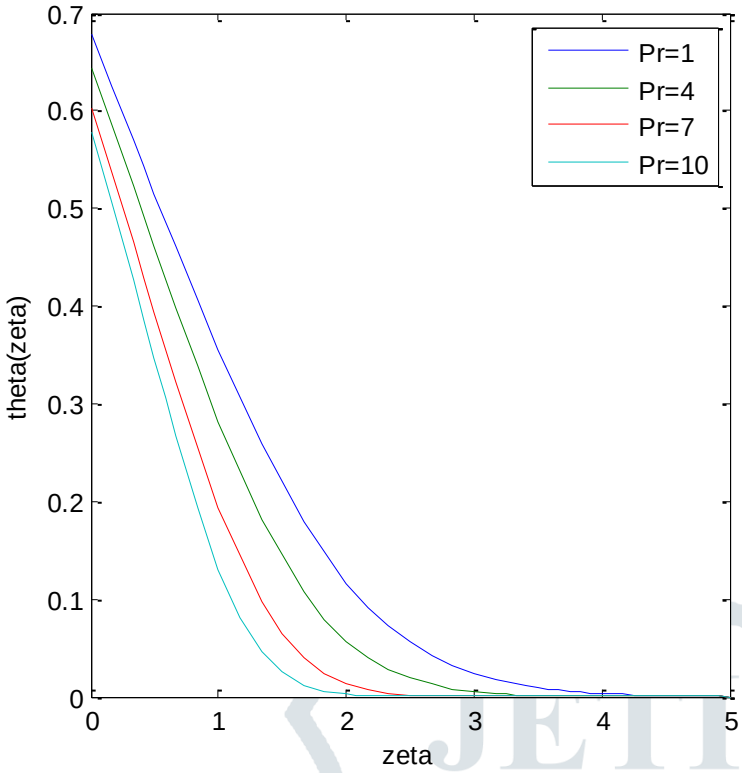

Figure 4.7 Temperature profile for different values of Prandtl number

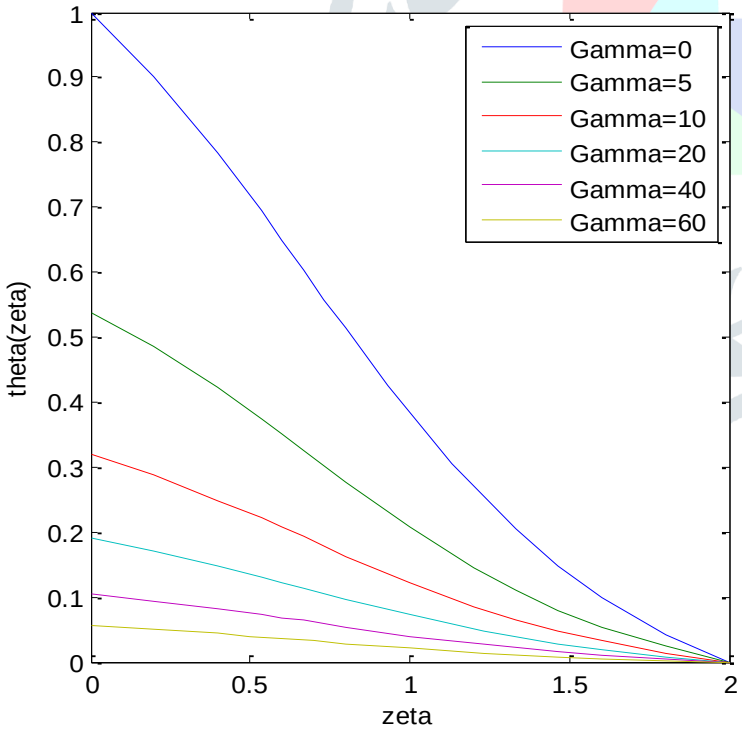

Figure 4.8 Temperature profile for different values of Thermal slip parameter

V RESULT AND DISCUSSION

Effects of varied non - dimensional parameter wall roughness (λ_1 and λ_1)in Newtonian and non - Newtonian fluid, Reiner - Rivlin fluid (K), Prandtl number(Pr), thermal slip (γ) on velocity and temperature profile are mentioned and examined graphically. Table 1 show the impact of wall

roughness parameters and comparing the computational results of radial wall stress $F''(0)$, azimuthal wall stress $G'(0)$ and entrainment velocity $F(\infty)$ by the numerical theme is formed by with obtainable study [3] within the Newtonian fluid case. It demonstrates that our numerical findings are nearly the same as those found by [3] for all values of wall roughness parameters.

Table 2 computes $F''(0), G'(0)$and $F(\infty)$ for numerous parameter values. In either radial or azimuthal slip coefficient incremented once torque furthermore because the skin friction factor elevates. The local Nusselt number obtained at completely different values of Reiner-Rivlin fluid parameter K and thermal slip parameter γ includes in table 3. It can increase elasticity parameter K then heat transfer rate ought to be elevate. The heat penetration depth shortens when thermal slip coefficient will increases and additionally Prandtl number Pr will increases once the heat transfer rate elevates. In figure 4.1 depicts the dimensionless velocity profile for various values of the wall roughness parameters λ_1 and λ_2 in Newtonian fluid case. It is detected that a rise in wall roughness parameters lead to decrease within the velocity profile.

In figure 4.2 illustrates the impact of wall roughness parameters λ_1 and λ_2 in Newtonian fluid case on the temperature profile. It shows that temperature component increases with a rise within the wall roughness parameters. In figure 4.3 the effect of Reiner – Rivlin fluid parameter K on temperature profile is shown. It is obvious that as K is enlarged, the temperature profile is magnified. In figure 4.4 for numerous values of Reiner – Rivlin fluid parameter K in no - slip case, its impact on temperature profile is illustrated. It is additionally clear that because the value of Reiner – Rivlin fluid parameters increases, the temperature profile also increases.

In figure 4.5 indicates the fact that increase in wall roughness parameters λ_1 and λ_2 in non - Newtonian fluid case decelerates fluid flow within the Velocity profile. In figure 4.6 for various values of wall roughness parameters λ_1 and λ_2 in non - Newtonian fluid case, its result on the temperature profile are illustrated. It is also clear that as the value of wall roughness parameters increases, the temperature profile also increases. In figure 4.7 the result of Prandtl number on temperature profile is shown. It is obvious that as Pr is accrued, the temperature profile is weakened. In figure 4.8 for various values of Thermal slip parameter, its effect on the temperature profile are illustrated. It is additionally clear that because the value of thermal slip parameter increases, the temperature profile decreases.

VI CONCLUSION

In this study elasticity and wall roughness effects in Partial slip flow and heat transfer of non - Newtonian fluid evoked by a rough porous rotating disk is studied in the presence of suction. The consequences of viscoelasticity and wall roughness are examined numerically. The numerical resolution for determination governing nonlinear ordinary differential equation is executed through Runge-Kutta fifth order technique.

The Reiner-Rivlin fluid parameter K is incremented once radially outward flow close to the disk developed by disk centrifugal impact decrease. Decelerates driving torque and skin friction factor are expect for increasing elastic effects. The result of torque and skin friction factor are

increasing by increasing wall roughness parameters λ_1 and λ_2. The slip effect becomes stronger once the entrainment velocity reduces.

Radial velocity profile decreases close to the disk and also the wall roughness parameters elevates. The temperature profile is reciprocally proportional to the wall roughness parameters. Thermal boundary layer elevates for Reiner-Rivlin fluid parameter K values increases. Thermal slip parameter will increases once the thermal boundary layer shrinks and heat transfer rate enhances. Elastic impact enhances temperature profile however decreases the magnitude of local Nusselt number.

VII ACKNOWLEDGEMENTS

The authors are thankful to the learned referee for suggestions to improve the paper.

VIII REFERENCES

[1] T. von Kármán, Über laminare und turbulente Reibung, Z. Angew. Math. Mech. ZAMM 1 (1921) 233–252.

[2] M. Turkyilmazoglu, Three dimensional MHD stagnation flow due to a stretchable rotating disk, Int. J. Heat Mass Transf. 55 (2012) 6959–6965.

[3] M. Turkyilmazoglu, P. Senel, Heat and mass transfer of the flow due to a rotating rough and porous disk, Int. J. Therm. Sci. 63 (2013) 146–158.

[4] T. Hayat, M. Rashid, M. Imtiaz, A. Alsaedi, Magnetohydrodynamic (MHD) flow of Cu-water nanofluid due to a rotating disk with partial slip, AIP Adv. 5 (2015), https://doi.org/10.1063/1.4923380, Article ID 067169.

[5] J.A. Khan, M. Mustafa, T. Hayat, A. Alsaedi, A revised model to study the MHD nanofluid flow and heat transfer due to rotating disk: numerical solutions, Neural Comput. Appl. (2016), https://doi.org/10.1007/s00521-016-2743-4.

[6] I. Mustafa, T. Javed, A. Ghaffari, Heat transfer in MHD stagnation point flow of a ferrofluid over a stretchable rotating disk, J. Molec. Liq. 219 (2016) 526–532.

[7] M. Mustafa, MHD nanofluid flow over a rotating disk with partial slip effects: Buongiorno model, Int. J. Heat Mass Transf. 108 (2017) 1910–1916.

[8] A. Ahmadpour, K. Sadeghy, Swirling flow of Bingham fluids above a rotating disk: an exact solution, J. Non-Newton. Fluid Mech. 197 (2013) 41–47.

[9] B. Sahoo, S. Poncet, Flow and heat transfer of a third grade fluid past an exponentially stretching sheet with partial slip boundary condition, Int. J. Heat Mass Transf. 54 (2011) 5010–5019.

[10] S. Han, L. Zheng, C. Li, X. Zhang, Coupled flow and heat transfer in viscoelastic fluid with Cattaneo-Christov heat flux model, Appl. Math. Lett. 38 (2014) 87–93.

[11] L. Zhang, C. Zhang, X. Zhang, J. Zhang, Flow and radiation heat transfer of a nanofluid over a stretching sheet with velocity slip and temperature jump in porous medium, J. Franklin Inst. 350 (2013) 990–1007.

[12] T. Javed, I. Mustafa, Slip effects on a mixed convection flow of a third-grade fluid near the orthogonal stagnation point on a vertical surface, J. Appl. Mech. Tech. Phys. 57 (2016) 527–536.

[13] D.S. Chauhan, A. Olkha, Slip flow and heat transfer of a second-grade fluid in a porous medium over a stretching sheet with power-law surface temperature or heat flux, Chem. Eng. Commun. 198 (2011) 1129–1145.

[14] S. Hina, M. Mustafa, T. Hayat, A. Alsaedi, Peristaltic flow of powell-eyring fluid in curved channel with heat transfer: a useful application in biomedicine, Comput. Meth. Prog. Biomed. 135 (2016) 89–100.

[15] S. Abbasbandy, M. Mustafa, T. Hayat, A. Alsaedi, Slip effects on MHD boundary layer flow of Oldroyd-B fluid past a stretching sheet: an analytic solution, J. Brazilian Soc. Mech. Sci. Eng. 39 (2017) 3389–3397